



# Switching characteristics of spin valve devices designed for MRAM applications

S.E. Russek<sup>a,\*</sup>, J.O. Oti<sup>a</sup>, Young K. Kim<sup>b</sup>

<sup>a</sup>National Institute of Standards and Technology mc 814.05, 325 Broadway, Boulder, CO 80303, USA

<sup>b</sup>MR Head Division, Samsung Electro-Mechanics Co., Seoul, South Korea

---

## Abstract

The low-frequency performance of spin valve giant magnetoresistive devices, designed for digital applications, has been examined as a function of device line width and aspect ratio. NiFe–Co–Cu–Co–NiFe–FeMn devices have been fabricated with line widths down to 0.4  $\mu\text{m}$  and aspect ratios that varied between 10:1 and 1.5:1. As the device line width decreases, the switching fields and switching field asymmetry increase due to magnetostatic effects. As the aspect ratio decreases, the switching field asymmetry increases rapidly and the devices become prone to domain noise. The experimentally observed switching behavior is compared to uniform rotation models to determine the accuracy with which the switching fields can be predicted. © 1999 Elsevier Science B.V. All rights reserved.

*Keywords:* MRAM; Spin-valve; Switching

---

Spin valve giant magnetoresistance devices have been proposed for digital applications such as magnetoresistive random access memory (MRAM) and digital recording heads [1–3]. These devices are similar to spin valves designed for analog sensor applications in that they have two conductive magnetic layers, a free and a pinned layer, separated by a thin conducting nonmagnetic spacer layer. The digital spin valve differs from the analog sensor in that the pinned layer is pinned along the long dimension of the device and the applied field is predominantly along the long dimension. This device configuration has only two stable states, parallel and antiparallel alignment of the magnetizations.

In this paper we describe how the magnetoresistive (MR) characteristics of the spin valve devices change as the dimensions are reduced below 1  $\mu\text{m}$  and when the aspect ratio is varied. In micromagnetic simulations, Zheng et al. [2] and Oti et al. [4] have shown that these devices will become asymmetric and susceptible to

domain noise as the dimensions and the aspect ratios are reduced. Gadbois et al. [5] have shown that the reversal process is very sensitive to the device shape and end profile. Their simulations indicate that in devices with square or blunt ends, the reversal process will be nucleated by vortices and closure domains at the device ends. The switching fields, in this case, are predicted to be substantially less than the switching fields predicted by uniform rotation models. The data presented in this paper, taken on devices with blunt ends, confirm that the switching fields are only 40% of the uniform rotation prediction. The dependence of the switching fields on device size and aspect ratio does, however, retain some of the qualitative features of single-domain rotation models.

The device structures consisted of Ta–NiFe–Co–Cu–Co–NiFe–FeMn–Ta multilayers sputtered on oxidized (1 0 0) Si substrates. The films were deposited in field to obtain an easy axis along the long dimension of the device and to set the pinning layer. The easy-axis anisotropy fields are typically  $\sim 0.4$  kA/m. The wafers were patterned to form bars with line widths varying from 16 to 0.4  $\mu\text{m}$  and aspect ratios varying from 10:1 to 1.5:1. The corners of the device ends are rounded by the

---

\* Corresponding author. Tel.: +1-303-497-5097; e-mail: russek@boulder.nist.gov.

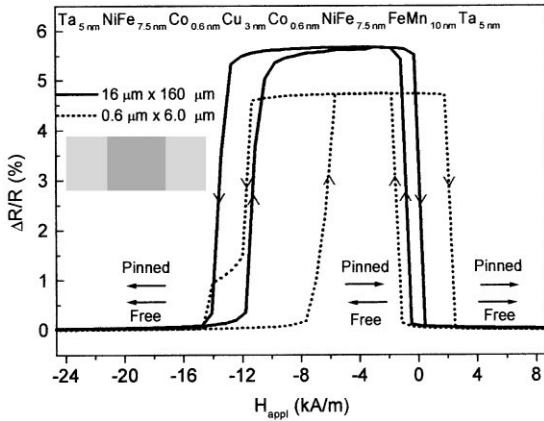


Fig. 1. MR response of 16 and 0.6  $\mu\text{m}$  wide devices with a 10 : 1 aspect ratio, showing the switching of the free and pinned layers. The horizontal arrows indicate the magnetic state in each different region. The inset shows a picture of a 0.8  $\mu\text{m}$  wide device.

lithographic and etching processes and yield devices with rounded ends as shown in the inset in Fig. 1. The active area, the region between the Au contact electrodes, was varied from one to eight squares. Typical MR response for field applied parallel to the long axis of the device, showing both the free and pinned layer switching, is shown in Fig. 1. The Cu layers in these devices are thick enough that there is little exchange coupling between the two magnetic layers. A small ferromagnetic coupling interaction ( $H_{\text{co}} \sim 0.4$  kA/m) in these devices can be measured by the free layer loop shifts on large devices which have minimal magnetostatic effects.

The effect of device line width is shown in Fig. 2 for devices with a 10 : 1 aspect ratio. The MR response,  $\Delta R/R$ , systematically decreases as the line width decreases. If it is assumed that the decrease in  $\Delta R/R$  is due to a dead zone of width  $\delta$  on both edges of the devices, then the data can be accurately fitted assuming a dead zone of width  $\delta = 55$  nm as shown in the Fig. 2 (inset). The MR response becomes sharper and the free layer switching fields increase as the line width is decreased. This is expected since the magnetostatic energy required for reversal of the free layer increases as the line width is decreased. If the free layer acts as a single-domain particle, which must switch by rotation, then the energy barrier height between the two states is proportional to the difference in the demagnetizing factors for the two directions parallel and perpendicular to the device stripe. For a large aspect ratio,  $A_{\text{R}} = L/w$ , where  $L$  and  $w$  are the device length and width, respectively, the barrier height is  $\Delta E \propto Mt/w$  where  $M$  and  $t$  are the magnetization and thickness of the free layer. The final effect is that the switching fields are asymmetric. This is due to the magnetostatic interaction between the free and pinned layers. The two layers are in a lower energy state when the

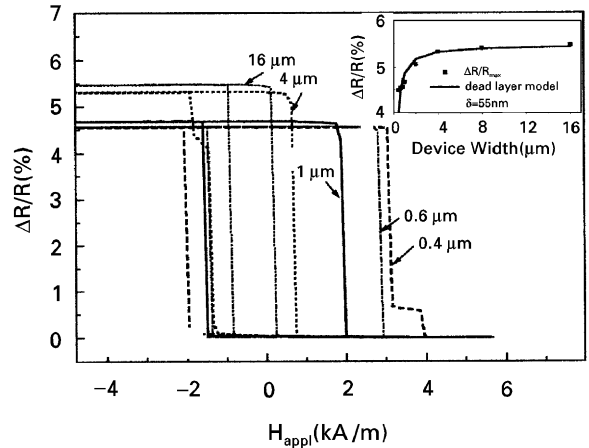


Fig. 2. MR response of devices with a 10 : 1 aspect ratio for line widths down to 0.4  $\mu\text{m}$ . The inset plots the decrease in  $\Delta R/R$  as a function of line width and a fit assuming a dead zone of width  $\delta = 55$  nm.

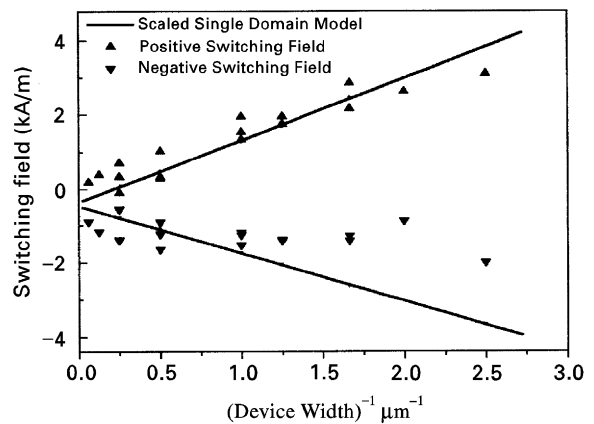


Fig. 3. Summary of the switching fields as a function of inverse line width for devices with a 10 : 1 aspect ratio. The solid line shows single-domain model data scaled by a factor of 0.4.

magnetizations are antiparallel. Therefore, switching from the antiparallel state (high resistance state) to the parallel state (low resistance state) requires a larger switching field. The switching field asymmetry is roughly proportional to the demagnetizing field of the pinned layer at the centre of the free layer which, for large aspect ratios, scales as  $H_{\text{d}} \propto 1/A_{\text{R}}^2 w$ .

The switching fields (defined as the midpoint of the resistive transitions) for devices with a 10 : 1 aspect ratio, as a function of inverse line width, are shown in Fig. 3. Also shown are scaled data from a multilayer single-domain rotation model [6]. This model maps the magnetic layers onto interacting single-domain particles of similar aspect ratio and incorporates magnetostatic

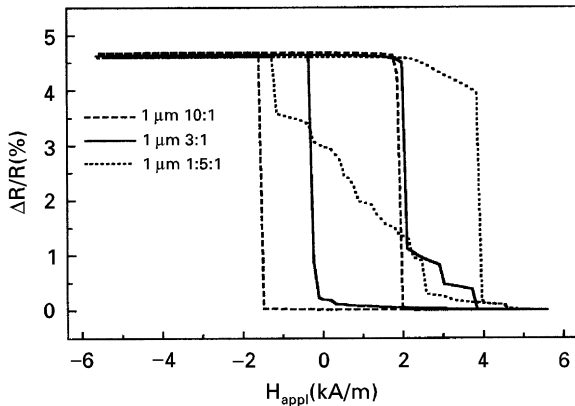


Fig. 4. MR response as a function of aspect ratio for devices with a  $1.0\ \mu\text{m}$  line width. The broad irregular resistive transitions, seen in the small aspect ratio devices, indicate complicated multidomain domain reversal processes.

interactions, exchange interactions, and magnetic anisotropy effects. The switching fields from the model calculations have been scaled by a factor of 0.4 to fit the experimental data. The positive switching fields, while only 40% of the single domain rotation values, still display a linear increase with inverse device width. The negative switching fields, however, show considerable divergence from the linear behavior. The large deviation in the values of the switching fields from the single-domain rotation models is consistent with the micromagnetic simulations which show a complicated reversal process nucleated from end domains.

As the aspect ratio decreases the difference in the self-demagnetizing energies decreases and the magnetostatic interactions between the layers increase. These effects lead to the reduction in the width of the hysteresis loops and to the increase in the switching field asymmetry (shift of the curves to the right) as seen in Fig. 4. For the smallest aspect ratio (1.5 : 1), where the magnetostatic interactions are largest, there is no longer a well-defined switching field. The device reverses through a complicated set of stable intermediate domain states. The complicated multidomain reversal is also seen in 3 : 1 devices with line widths below  $1\ \mu\text{m}$ . The beginning of multidomain reversal is seen in the magnetoresistive response of the 3 : 1 device shown in Fig. 4. Fig. 5 shows a summary plot of the switching fields for 3 : 1 aspect ratio devices. The model data is again scaled by a factor of 0.4 to fit the data. As with the 10 : 1 devices, there is a clear deviation,

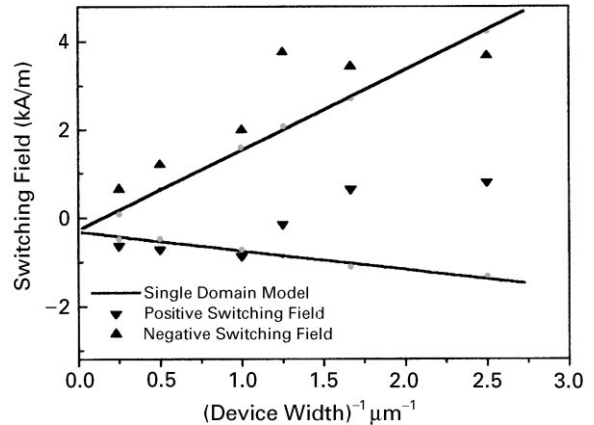


Fig. 5. Summary of the switching fields as a function of inverse line width for devices with a 3 : 1 aspect ratio. The solid line shows single-domain model data scale by a factor of 0.4.

at small line widths, of the negative switching fields from the linear behavior predicted by the uniform rotation model. For 3 : 1 aspect ratio devices, however, the deviation from the model more clearly coincides with domain structure effects seen in the resistive transition.

From an applications standpoint, the response of the 10 : 1 devices is encouraging. The devices show sharp switching response which is characteristic of an ideal two-state system. The deviation from uniform rotation behavior may be a problem for applications since the switching fields and their scaling behavior are hard to predict. The non-rotational switching process may also present problems with the reproducibility of switching of individual devices [7] and the uniformity of switching in large ensembles of devices.

## References

- [1] D.D. Tang, P.K. Wang, V.S. Speriosu, S. Le, K.K. Kung, IEEE Trans. Magn. 31 (1995) 3206.
- [2] Y. Zheng, J.-G. Zhu, IEEE Trans. Magn. 32 (1996) 4237.
- [3] X. Che, US Patent No. 5,546,253, 1996.
- [4] J.O. Oti, S.E. Russek, IEEE Trans. Magn. 33 (1997) 3298.
- [5] J. Gadbois, J.-G. Zhu, W. Vavra, A. Hurst, IEEE Trans. Magn. 34 (1998) 1066.
- [6] J.O. Oti, R.W. Cross, S.E. Russek, Y.K. Kim, J. Appl. Phys. 79 (1996) 6386.
- [7] B.A. Everitt, A.V. Pohm, R.S. Beech, A. Fink, J.M. Daughton, IEEE Trans. Magn. 34 (1998) 1060.